



Research article

Evaluation of RevX solution extract as a potential inhibitor of the main protease of SARS-CoV-2—*In vitro* study and molecular dockingFeng-Pai Chou^{a,b}, Chia-Chun Liu^c, Huynh Nguyet Huong Giang^d, Sheng-Cih Huang^a, Hsiu-Fu Hsu^{c,*}, Tung-Kung Wu^{a,b,**}^a Department of Biological Science and Technology, National Yang Ming Chiao Tung University, 1001 Ta-Hsueh Rd., Hsinchu 30010, Taiwan, ROC^b Center for Emergent Functional Matter Science, National Yang Ming Chiao Tung University, 1001 Ta-Hsueh Rd., Hsinchu 30010, Taiwan, ROC^c Department of Chemistry, Tamkang University, No.151, Yingzhuang Rd., Tamsui Dist., New Taipei City 251301, Taiwan, ROC^d Department of Material Science, National Yang Ming Chiao Tung University, 1001 Ta-Hsueh Rd., Hsinchu 30010, Taiwan, ROC

HIGHLIGHTS

- The unique substrate specificity of SARS-CoV-2 M^{Pro} makes it a potential target for drug design.
- Fermented sorghum extract RevX solution enhances adjuvant therapy of lung adenocarcinoma, suggesting the role of bioactive components in RevX solution.
- The solid extract of RevX showed potent M^{Pro} inhibitory activity with IC₅₀ of 2.07 ± 0.38 µg/mL.
- The three sterol-like structures of RevX extract showed a similar binding cavity to Mpro-GC376, suggesting its putative inhibitory activity.

ARTICLE INFO

Keywords:

Sorghum

Sterol

M^{Pro}

GC-376

Antiviral drug

ABSTRACT

The main protease (M^{Pro}) of SARS-CoV-2 is a protease necessary for viral polyprotein processing and maturation. M^{Pro} cleaves the polypeptide sequence after the glutamine residues. There is no known cellular protease with this substrate specificity in humans; therefore, it is considered an attractive drug target. Previously, fermented sorghum extract RevX (trademark of Revoltrix INC.) solution significantly alleviated physical decline and complications in a patient with lung adenocarcinoma, suggesting the role of bioactive components in RevX solution. To further explore whether the bioactive components in RevX solution exhibit other biological activities, such as antiviral effects, we investigated its inhibitory effect on the M^{Pro} of SARS-CoV-2 virus. We report herein that the solid extract of the RevX solution exhibits an efficacious M^{Pro} inhibitory activity, with IC₅₀ of 2.07 ± 0.38 µg/mL. Molecular docking of sterol-like components in the RevX extracts identified by MS shows that the three sterol-like molecules can bind to the active region of the GC376-M^{Pro} complex, supporting the structure-function relationship. Combined with its ability to significantly alleviate the body's immunity decline and to inhibit the activity of SARS-CoV-2 M^{Pro}, RevX solution may provide a possible alternative supportive treatment for patients with COVID-19.

1. Introduction

The 2019 global pandemic coronavirus disease (COVID-19), caused by severe acute respiratory syndrome-related coronavirus-2 (SARS-CoV-2), has caused high morbidity and mortality, and severe social, economic, and political chaos. As of 16 November 2021, the number of confirmed cases has exceeded 253.26 million, and the death toll has surpassed 5.11 million (<https://sites.google.com/cdc.gov.tw/2019ncov/global>). SARS-

CoV-2 belongs to the *Coronaviridae* family and is a member of the same family as SARS-CoV for severe acute respiratory syndrome and MERS-CoV for the Middle East respiratory syndrome (Gordon et al., 2020). SARS-CoV-2, SARS-CoV and MERS-CoV viruses are all enveloped positive-stranded single-stranded RNA viruses. Phylogenetic analysis of the original SARS-CoV-2, SARS-CoV and MERS-CoV genomes showed that both SARS-CoV and SARS-CoV-2 are members of the genus *Beta-coronavirus* and the subgenus *Sarbecovirus* (beta-CoV lineage B), whereas

* Corresponding author.

** Corresponding author.

E-mail addresses: hhsu@mail.tku.edu.tw (H.-F. Hsu), tkwmll@nycu.edu.tw (T.-K. Wu).<https://doi.org/10.1016/j.heliyon.2022.e09034>

Received 26 November 2021; Received in revised form 8 February 2022; Accepted 24 February 2022

2405-8440/© 2022 The Authors. Published by Elsevier Ltd. This is an open access article under the CC BY-NC-ND license (<http://creativecommons.org/licenses/by-nc-nd/4.0/>).

MERS-CoV is a member of the subgenus *Merbecovirus* (beta-CoV lineage C). The sequence identity between SARS-CoV-2 and SARS-CoV and MERS-CoV is approximately 79% and 50%, respectively. In addition, both SARS-CoV-2 and SARS-CoV enter host cells by binding to angiotensin-converting enzyme 2 (ACE 2), while MERS-CoV enters host cells by binding to dipeptidyl peptidase 4 (DPP4) receptors (Ge et al., 2013; Fehr and Perlman, 2015; Lu et al., 2020). The genome of SARS-CoV-2 is about 30 kb in size and contains 16 open reading frames (ORFs) (Lu et al., 2020). Among them, the replicase gene (ORF 1ab) encodes for the two overlapping polyproteins pp1a and pp1ab, which are cleaved by the main protease (M^{pro} , also referred to as 3CL pro) (Figure 1) (Ullrich and Nitsche, 2020; Yang and Rao, 2021). This is a key step in the process of virus replication, transcription, and maturation (Du et al., 2004). Additional genome contains accessory and structural proteins such as envelope protein (E), membrane protein (M), nucleocapsid phosphoprotein (N), and spike glycoprotein (S). The functional role of spike glycoprotein S involves host tropism and hopping, and enters the cell by recognizing the ACE 2 receptor (Du et al., 2009). So far, although several vaccines with effective immunity have been claimed, breakthrough infections still occur. Several drugs, including remdesivir (Saha et al., 2020), molnupiravir (MK-4482, EIDD-2801) (Painter et al., 2021), glycyrrhetic acid (Ding et al., 2020) and vitamin D (Grant et al., 2020) have been tested under clinical trials for COVID-19 treatment. However, safe and effective drugs and supportive treatments are still needed to combat with the current COVID-19 pandemic (Li and Clercq, 2020).

Among the putative therapeutic targets for the treatment of COVID-19, the main protease (M^{pro}) is often a potential drug target (Hartenian et al., 2020). Inhibiting the activity of M^{pro} can reduce the assembly of mature virus particles during the process of viral polyprotein processing and maturation, thereby achieving the key function of virus infection resistance. The structure of SARS-CoV-2 M^{pro} was recently solved by Zhou et al. at pH7 (Zhang et al., 2020a,b). M^{pro} is a functional dimer and cysteine protease with a histidine-cysteine catalytic dyad at the active site (Ullrich and Nitsche, 2020). The protease has a unique substrate preference for glutamine at the P1 position of the polyprotein (Leu-Gln↓(Ser, Ala, Gly)) and, specifically, cleaves the peptide sequence after the glutamine residues (Rut et al., 2021). There is no known cellular protease with such substrate specificity in humans (Hilgenfeld, 2014; Zhang et al., 2020a,b). Therefore, inhibiting the function of M^{pro} can block the replication of coronaviruses without affecting human host cells, which makes M^{pro} inhibitors promising candidates for the treatment of patients with coronavirus infection. Until now, there have been few reports on safe and effective M^{pro} inhibitors, leaving an urgent need to

discover more M^{pro} inhibitors to develop as therapeutic agents against COVID-19.

Phytochemicals in medicinal plants are known to be a major source of lead compounds for drug development (Egbuna et al., 2020). It has been reported that some natural products (such as alkaloids, flavonoids, polyketides, simple aromatics, terpenes, steroids, and phenolic compounds) have M^{pro} inhibitory activity, which encourages us to find more effective SARS-CoV-2 M^{pro} inhibitors from natural resources (Chojnacka et al., 2020; Russo et al., 2020; Wen et al., 2007). Sorghum contains low digestible proteins, unsaturated organics, and certain minerals, vitamins, phenols, terpenes, sterols, and fat-soluble compounds, and is an important source of nutrients and bioactive compounds in human and animal diets (Cardoso et al., 2017 and references therein). Sorghum from different sources shows a variety of biological activities, such as anti-oxidation, scavenging free radicals, anti-cancer, cardiac prevention, antimicrobial, antiviral, anti-diabetic, and neuroprotective abilities (Cardoso et al., 2017; Kamath et al., 2007; Muriu et al., 2002; Shih et al., 2007; Yang et al., 2009). For example, four compounds detected in *Sorghum bicolor* may reduce the severity of type-2 diabetic mellitus (T2DM) by activating the PPAR signaling pathway (Oh et al., 2020). Many studies have also shown that sorghum fermentation can increase the concentration and structural diversity of vitamins, phenols, terpenes, sterols, and fat-soluble compounds (Cardoso et al., 2017 and references therein).

RevX (trademark of Revolutr INC.) solution extract is a fermented extract of sorghum obtained by a unique extraction technology. It contains various compositions such as organic acids, sulfonamides, phytosterols, and anti-inflammatory ingredients. Previously, the RevX solution has been used as an adjuvant treatment for lung adenocarcinoma (Lin, 2021). For example, a 71-year-old woman supplemented with the RevX solution during targeted therapy experienced a significantly alleviated decline in physical strength during the study treatment period and greatly reduced her complications. This suggests that the RevX solution may be used as an adjuvant therapy for patients with metastatic lung adenocarcinoma. Given the effects of the bioactive components in RevX solution on improving mental and physical strength and reducing complications arising from targeted cancer treatment, it is worth exploring whether the bioactive components in RevX solution exhibit other biological activities, such as antiviral effects. In this study, we further explored whether the bioactive components in the RevX solution have inhibitory effects on the M^{pro} of the SARS-CoV-2 virus. Three extracts of RevX solution, solid, organic, and water, were first partially characterized using gas chromatography-mass spectrometry (GC-MS) and then

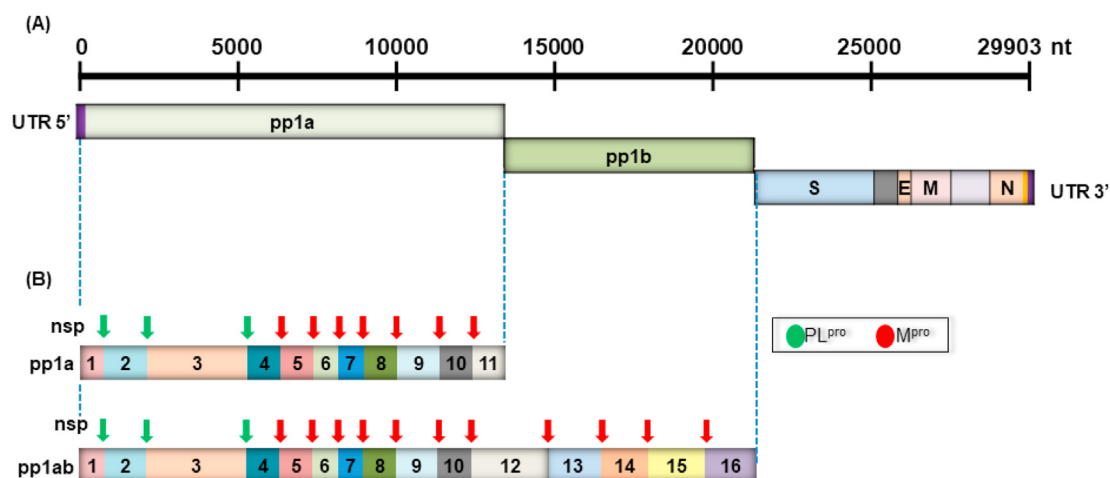


Figure 1. SARS-CoV-2 genome organization. (A) SARS-CoV-2 genomic RNA, encoding non-structural proteins (NSPs), ORF 1ab which can be directly translated into two polyproteins pp1a and pp1b, and structural and accessory proteins. (B) Schematic representation of non-structural polyprotein cleavage sites. Two viral proteases, a papain-like protease (PL pro , green arrow) and a main protease (M pro , red arrow), cleave the two polyproteins to generate 16 NSPs (Ullrich and Nitsche, 2020). The M pro recognizes and cleaves the virus non-structural polyprotein at 11 sites. The PL pro cleaves the virus non-structural polyprotein at 3 sites.

analyzed for SARS-CoV-2 M^{pro} inhibitory activity *in vitro*. The *in vitro* M^{pro} inhibitory activities of solid, organic, and water fractions showed IC₅₀s of 2.07 ± 0.38, 28.17 ± 3.49, and 32.73 ± 1.06 µg/mL, respectively. We then used molecular docking methods to search for compounds identified by MS that might interact with M^{pro}, hoping to link their possible structure-activity relationship to M^{pro} inhibition. Interestingly, three MS-identified sterol-like components were found in the active region of the GC376-M^{pro} complex, a potent M^{pro} inhibitor, suggesting that they may have a potential function to inhibit M^{pro} activity. Collectively, these results suggest that the RevX solution may be useful as an adjunctive treatment for patients with SARS-CoV-2 infection and to help COVID-19 patients recover quickly.

2. Materials and methods

2.1. The RevX solution extracts

The RevX solution extracts were obtained according to the following procedures. First, 600 mL of RevX solution was gently removed the solvent by rotary evaporation to obtain the solid (S) fraction. By dissolving it in 30 mL CCl₄ and 30 mL ddH₂O, the solid extract (S) was used to prepare the water (W) or organic (L) fractions using the following procedure: Collect the first organic layer (L1), add 30 mL of CCl₄ to the water layer, repeat the extraction, and collect the organic layer (L2). Then add 30 mL of water for extraction and repeat the above process again to collect the organic layer (L3). After collecting the organic layer, the remaining water layer was marked as W1, and add 30 mL of water to L1 + L2 + L3 for extraction, and collect the water layer as W2. Then, add 30 mL of water for extraction and repeat the above process to obtain W3. Removing the organic solvent in L1 + L2 + L3 and the water in W1 + W2 + W3 to obtain the organic (L) and water (W) extracts. The three different samples, solid part (S), organic part (L), and water-soluble part (W), were used for *in vitro* M^{pro} inhibitory activity determination experiments.

2.2. GC-MS analysis

GC-MS analysis was performed using an Thermo Trace 1300GC + ISQ MS instrument equipped with a Rxi-5MS (30 m × 0.25 mm × 0.25 µm) capillary column. The instrument was initially set at 50 °C, then ramped up to 300 °C at a rate of 10 °C/min, then held at 300 °C for 10 min. The inlet temperature was set at 300 °C. The column uses helium as the carrier gas, which is flowed at a constant rate of 1 mL/min. Electron ionization was performed with an electron beam at 70 eV. The split mode for sample injection is 5:1. The MS scan range was from *m/z* 35 to 600. Mass spectra of all detected compounds and fragmentation modes were compared with spectra libraries in NIST2017 + Wiley 10th Ed. The percentage of each compound is based on the relative peak area of each compound in the chromatogram.

2.3. In vitro inhibitory activity assay of M^{pro}

Dabcyl-KTSAVLQ↓SGFRKME-Edans is a Förster resonance energy transfer (FRET)-based 12-amino acid fluorescence quenching peptide that can be recognized and cleaved by M^{pro} (cleavage site: ↓) (Chen et al., 2006). The measurement of SARS-CoV-2 M^{pro} inhibition was performed according to the manufacturer's protocol with minor modifications (Zhang et al., 2020a,b). In short, the reaction was performed in a 384-well black flat-bottomed microtiter plate (Thermo Scientific™ Nunc™), with a final volume of 25 µL per well. The blank contained a 10 µL assay buffer (20 mM Tris, 100 mM NaCl, 1 % DTT, 1 % EDTA) and 2.5 µL inhibitor buffer (70% ethanol in water). The positive control contained a 10 µL M^{pro} protease in the assay buffer (36 nM, final concentration) and a 2.5 µL inhibitor buffer (70% ethanol in water). The inhibitor control contained a 10 µL M^{pro} protease and a 2.5 µL GC376 (1, 000 µM). The test samples of water and lipid fractions contained 10 µL M^{pro} protease and 2.5 µL of different concentrations of extract (0, 3.125,

6.25, 12.5, 25.0, 50.0, and 100.0 µg/mL). For the solid fraction, 2.5 µL of different concentrations of extracts (0, 0.78, 1.56, 3.125, 6.25, 12.5, and 25.0 µg/mL) was used. The reaction was initiated by incubating at 37 °C with slow shaking for 30 min. A 12.5 µL (40 µM, final concentration) substrate solution was added to start the hydrolysis reaction and was incubated at 37 °C for 1 h with slow shaking. The hydrolyzed product emitted a strong fluorescence signal (excitation/emission, 355 nm/460 nm) around 460 nm, which was recorded by a microplate reader (Fluoroskan Ascent FL, Thermo Fisher). The inhibitory effect was calculated by comparing with the control wells without an inhibitor. The IC₅₀ value was determined by nonlinear regression (GraphPad Prism 8.0.1). For the calculation, the enzyme activity was assumed to be 100%. The reaction was carried out in triplicate.

2.4. Molecular docking

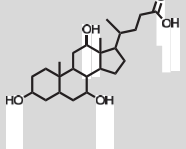
Ligand-based molecular docking of MS-identified RevX-extracted compounds with M^{pro} protein was performed using iGEMdock software to search for potential drug targets (Hsu et al., 2011). Briefly, iGEMdock is a structure-based virtual screening (VS) framework based on pharmacological interactions between ligands and targets. It integrates processes including ligand and binding site preparation, virtual screening, post-screening analysis, and pharmacological interactions. First, a screening compound and a binding site of interest are prepared. Then, using the in-house docking tool Gemdock, the compound is docked to the binding site. Next, iGEMdock uses hydrogen bonding (H), electrostatic (E), and van der Waals (V) interactions to generate protein-compound interaction profiles. Next, iGEMdock screened compounds for post-screen analysis using pharmacological interactions and clustering. Pharmacological interactions occur at conserved interacting residues that perform essential functions of target proteins by forming binding pockets with specific physico-chemical properties. Finally, iGEMdock combines the pharmacological interaction and energy-based scoring capabilities of Gemdock to perform hierarchical clustering dendrograms for screening, analysis, ranking, and visualization of screened compounds. The three-dimensional (3D) structure of SARS-CoV-2 M^{pro} was retrieved from the Protein Data Bank (<https://www.rcsb.org/structure/6W63>) in pdb format. Some ligand structures were obtained from the PubChem website (<http://pubchem.ncbi.nlm.nih.gov>), and the sdf format file was converted to Mol using Open Babel. Other ligands were drawn with ChemDraw 12.0 software and converted into Mol files with the ChemBio3D Ultra software. For docking experiments, amino acid residues, including His41, Cys44, Leu141, Asn142, Gly143, Ser144, Cys145, His163, His164, Met165, Glu166, Arg188, and Gln189 were used as active sites. The docking conformation of the ligand was determined by selecting the posture with the highest free energy of binding. The structural analysis of the system and graphics were carried out using PyMOL2 (Accelrys Software Inc., San Diego, CA, USA) and Ligplot + v.2.2.4 (DeLano, 2002).

3. Results and discussion

3.1. RevX extracts fractionation and GC-MS analysis

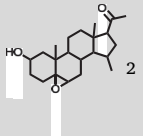
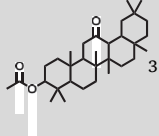
The RevX solution was concentrated by a rotary evaporator and was drained directly and extracted with carbon tetrachloride (CCl₄) and distilled water (ddH₂O) to obtain three parts: solid (S), organic (L), and water (W) fractions. Gas chromatography–mass spectrophotometry (GC-MS) was applied to identify the main components of each fraction. From the GC-MS process, more than 300 compounds were separated from the RevX solution extracts, and 80 main components were identified. The GC-MS analysis results show that representative components were identified, including flavonoids, vitamins, phenols, terpenes, sterols, and fat-soluble compounds. Based on the purpose of this study to focus on sterol-like components, Table 1 shows the representative compounds with sterol-like structures identified in the RevX solution extracts using GC-MS. All 13 compounds were screened for physio-chemical

Table 1. Representative sterol-like components identified by MS obtained from the RevX solution extract.

| Name | Chemical formula | Molecule name | Chemical structure | Retention Time (min) |
|------|---|---|---|----------------------|
| J1 | C ₃₀ H ₅₀ O ₂ | 3 α -(hydroxymethyl)-5 α ,5 β ,8,8, 11 α -pentamethyl-1-prop-1-en-2-yl-1,2,3,4,5,6,7,7 α ,9,10,11,11b, 12,13,13 α ,13 β -hexadeca hydrocyclopenta [α]chrysen-9-ol |  | 32.94 |
| J2 | C ₁₉ H ₂₄ | 1,1-dimethyl-6-(propan-2-yl)-1,2,3,4-tetrahydrophenanthrene |  | 20.13 |
| J3 | C ₂₉ H ₅₀ O | (3S)-17-(5-ethyl-6-methylheptan-2-yl)-10,13-dimethyl-2,3,4,7,8,9, 11,12,14,15,16,17-dodecahydro-1H-cyclopenta [α]phenanthren-3-ol |  | 20.67 |
| J4 | C ₂₄ H ₄₀ O ₅ | (4R)-4-((3S,5S,7R,8R,9S,10S,12S,13R,14S,17R)-3,7,12-trihydroxy-10,13-dimethyltetradecahydro-1H-cyclopenta [α]phenanthren-17-yl)pentanoic acid |  | 21.81 |
| J5 | C ₃₂ H ₅₂ O ₃ | (13 α ,14 β ,17 α)-3 β -(acetyloxy)-5 α -lanost-8-en-7-one |  | 26.84 |
| J6 | C ₃₀ H ₅₂ O ₂ | 7,7,12,16-tetramethyl-15-(6-methylheptan-2-yl)pentacyclo [9.7.0.0 ^{1,3} .0 ^{3,8} .0 ^{12,16}]octadecane-6,10-diol |  | 25.82 |
| J7 | C ₃₂ H ₅₂ O ₃ | 24,25-epoxylanost-8-en-3-ol acetate |  | 26.84 |
| J8 | C ₂₁ H ₂₉ NO ₃ S | 19-methoxy-9,13-dimethyl-20-thia-18-azapentacyclo [10.5.3.0 ^{1,13} .0 ^{4,12} .0 ^{5,9}]icos-18-ene-8,16-dione |  | 25.70 |
| J9 | C ₃₀ H ₅₀ O | (1R,3 α R,5 α R,5 β R,7 α R,9S,11 α R,11 β R,13 α R,13 β R)-3 α ,5 α ,5 β ,8,8, 11 α -hexamethyl-1-prop-1-en-2-yl-1,2,3,4,5,6,7,7 α ,9,10,11,11b, 12,13,13 α ,13 β -hexadecahydro cyclopenta [α]chrysen-9-ol |  | 27.42 |
| J10 | C ₁₉ H ₂₄ O ₃ | 12- α -hydroxyandrosta-1,4-diene-3,17-dione |  | 28.03 |
| J11 | C ₂₇ H ₄₄ O ₃ | (6R)-6-((1R,3 α S,4E,7 α R)-4-((2Z)-2-((5S)-5-hydroxy-2-methylenecyclohexylidene)ethylidene)-7 α -methyl-2,3,3 α ,5,6,7-hexahydro-1H-inden-1-yl]-2-methylheptane-2,3-diol |  | 23.22 |

(continued on next page)

Table 1 (continued)

| Name | Chemical formula | Molecule name | Chemical structure | Retention Time (min) |
|------|--|--|---|----------------------|
| J12 | C ₂₂ H ₃₄ O ₃ | 1-(4-hydroxy-2,13,16-trimethyl-8-oxapentacyclo [9.7.0.0 ^{2,7} .0 ^{7,9} .0 ^{12,16}]octadecan-15-yl)ethanone |  | 23.61 |
| J13 | C ₃₂ H ₅₂ O ₃ | 4,4,6α,6β,8α,11,11,14β-octamethyl-13-oxodocosahydricen-3-yl acetate |  | 26.84 |

characteristics, drug-likeness properties, and bioavailability scores by Lipinski's rule using SwissADME analysis (Lipinski et al., 2011). As shown in Table 2, all 13 compounds met Lipinski's rule and had a satisfactory "Abbott Bioavailability Score (>0.1)".

Table 2. Physico-chemical properties of the 13 sterol-like compounds for drug-likeness and bioavailability score^a.

| Name | Lipinski's rules | | | | | Bioavailability score |
|------|------------------|---------|--------|--------------|--------------------------|-----------------------|
| | MW ≤500 | HBA <10 | HBD ≤5 | Mlog P ≤4.15 | Lipinski's violations ≤1 | |
| J1 | 442.72 | 2 | 2 | 6.00 | 1 | 0.55 |
| J2 | 252.39 | 0 | 0 | 6.19 | 1 | 0.55 |
| J3 | 414.71 | 1 | 1 | 6.73 | 1 | 0.55 |
| J4 | 408.57 | 5 | 4 | 3.05 | 0 | 0.56 |
| J5 | 484.75 | 3 | 0 | 6.10 | 1 | 0.55 |
| J6 | 444.73 | 2 | 2 | 6.14 | 1 | 0.55 |
| J7 | 484.75 | 3 | 0 | 6.20 | 1 | 0.55 |
| J8 | 375.19 | 4 | 0 | 3.03 | 0 | 0.55 |
| J9 | 426.72 | 1 | 1 | 6.92 | 1 | 0.55 |
| J10 | 300.39 | 3 | 1 | 2.53 | 0 | 0.55 |
| J11 | 416.66 | 3 | 3 | 4.33 | 1 | 0.55 |
| J12 | 346.50 | 3 | 1 | 3.49 | 0 | 0.55 |
| J13 | 484.75 | 3 | 0 | 6.20 | 1 | 0.55 |

^a MW, molecular weight (g mol⁻¹); HBA, hydrogen bond acceptor; HBD, hydrogen bond donor; log P, lipophilicity; bioavailability score, a determinant of oral absorption of drug or other substances.

3.2. Mpro inhibitory activity assay

Three RevX extracts, solid (S), organic (L), and water (W) fractions, were studied *in vitro* against M^{Pro} in a spectrofluorometric assay. A novel fluorescent peptide, Dabcyl-KNSTLQSGLRKE-Edans, was used as a substrate for Förster resonance energy transfer (FRET). GC376, a cysteine

protease inhibitor that specifically binds to Cys145 of M^{Pro} with a potent *in vitro* inhibitory concentration of 80 nM, was used as an inhibitor control (Vuong et al., 2020). The three fractions with a final concentration of 50 µg/mL were initially used in the M^{Pro} inhibition test, and the emission fluorescence intensity detected at wavelength 460 nm was compared with the GC376 inhibitor control experiment. The results showed that, compared with GC376, the inhibitory activity of the enzyme exceeded 50%. To further quantify the inhibitory activity, different doses (from 0.0 to 100.0 µg/mL) were used to draw the dose-inhibition curve of the three fractions of M^{Pro}. As shown in Figure 2, the solid, organic, and water fractions inhibit the target enzyme in a dose-dependent manner, and the calculated IC₅₀ values were 2.07 ± 0.38 µg/mL, 28.17 ± 3.49 µg/mL, and 32.73 ± 1.06 µg/mL, respectively. This finding indicates that all three fractions contain naturally occurring inhibitors against SARS-CoV-2 M^{Pro}, with the solid fraction showing the strongest inhibitory effect.

3.3. Molecular docking of RevX extract components identified by MS with M^{Pro}

Molecular docking, a method for predicting the preferred binding affinity and mode of a ligand to proteins of known three-dimensional structure, has become one of the most popular methods for drug discovery (Meng et al., 2011). To correlate the structure-function relationship of M^{Pro} inhibition with the RevX extract, a docking simulation of the components of the RevX extract identified by MS and M^{Pro} was performed and compared with the crystal structure of the M^{Pro}-GC376 complex (Kneller et al., 2020). Previously, Vuong et al. reported the X-ray structure of the SARS-CoV-2 M^{Pro}-GC373 and M^{Pro}-GC376 complexes (Vuong et al., 2020). GC373 is the aldehyde form of GC376 and is covalently bound to Cys145 (Vuong et al., 2020). Molecular docking and X-ray structure of the GC376-M^{Pro} complex exhibited similar active site cavity packing and electrostatic or hydrogen bonding interactions between amino acid residues and ligands (Figure 3). The glutamine surrogate of GC376 (P1 position) forms H-bonds with His163 and Glu166 and hydrophobic interactions with His172. The Leu of GC376 (P2 position)

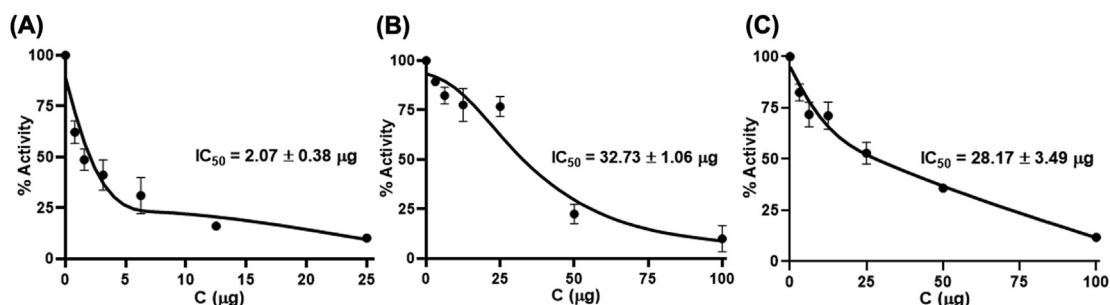


Figure 2. The inhibitory activity of SARS-CoV-2 M^{Pro} in serial dilutions of (A) solid, (B) organic, and (C) water fractions.

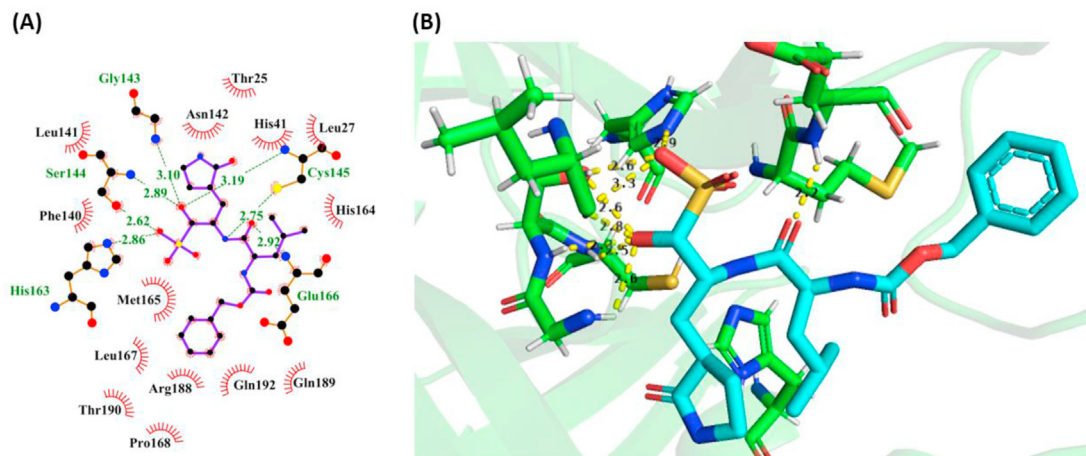


Figure 3. Molecular docking of GC376 and SARS-CoV-2 M^{PRO}. (A) Ligplot image showing both hydrogen and hydrophobic interactions by GC376 and M^{PRO}, and (B) Docking pose of GC376 against M^{PRO}.

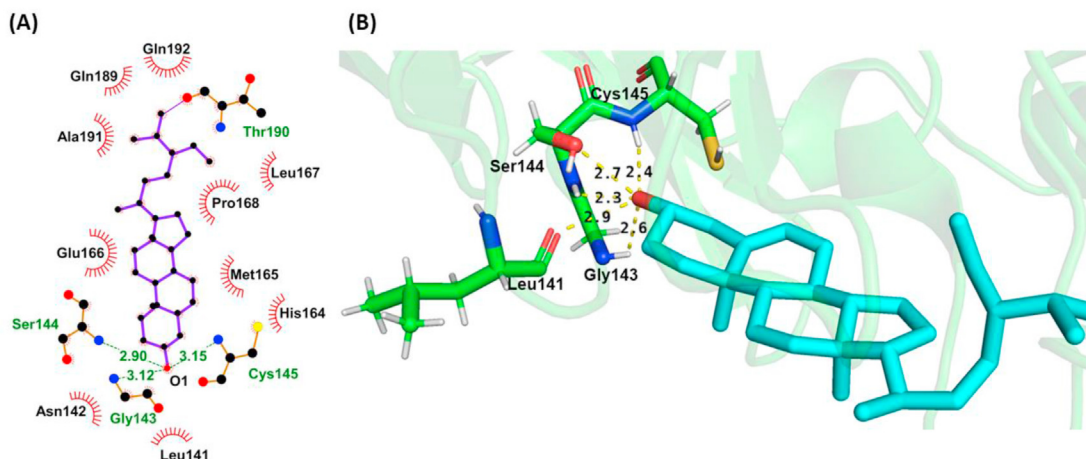


Figure 4. Molecular docking of J3 and SARS-CoV-2 M^{PRO}. (A) Ligplot image showing both hydrogen and hydrophobic interactions by J3 and M^{PRO}, and (B) Docking pose of J3 against M^{PRO}.

inserted into the S2 hydrophobic pocket consisting of Arg40, His41, Cys44, Met49, Tyr54, Met165, Arg188 and Gln189. The benzyl ring of GC376 (P3 position) fits into the S1 binding site and forms a H-bond with the side chain carboxyl group of Glu166. The hydrophobic and hydrogen bonding interactions of these residues form a support for drug binding

(Fu et al., 2020). The backbones of Gly143, Ser144, and Cys145 form the oxyanion hole. Previously, the flexibility of M^{PRO} was as pH-dependent as SARS-CoV M^{PRO} (Tan et al., 2005). Proteins were found to be most stable at neutral pH. Basic protein structures become the most unstable with changes in pH, and acidic pH also tended to alter the structural properties

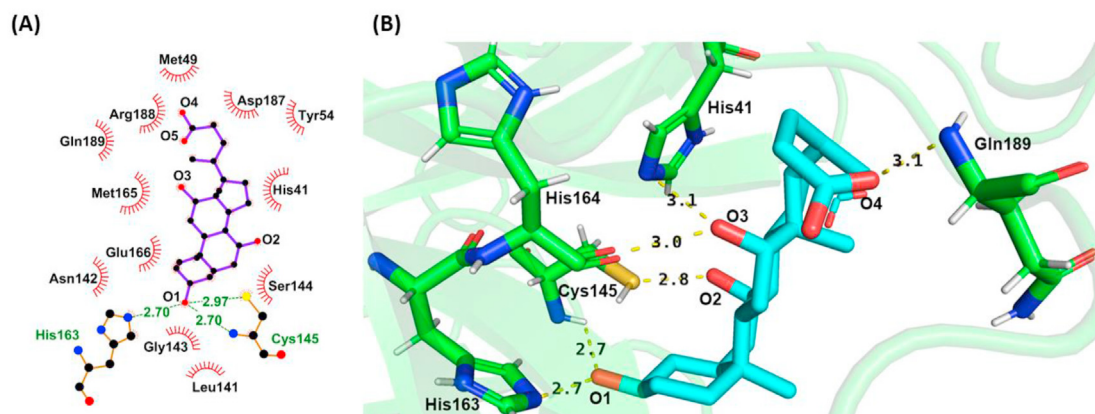


Figure 5. Molecular docking of J4 and SARS-CoV-2 M^{PRO}. (A) Ligplot image showing both hydrogen and hydrophobic interactions by J4 and M^{PRO}, and (B) Docking pose of J4 against M^{PRO}.

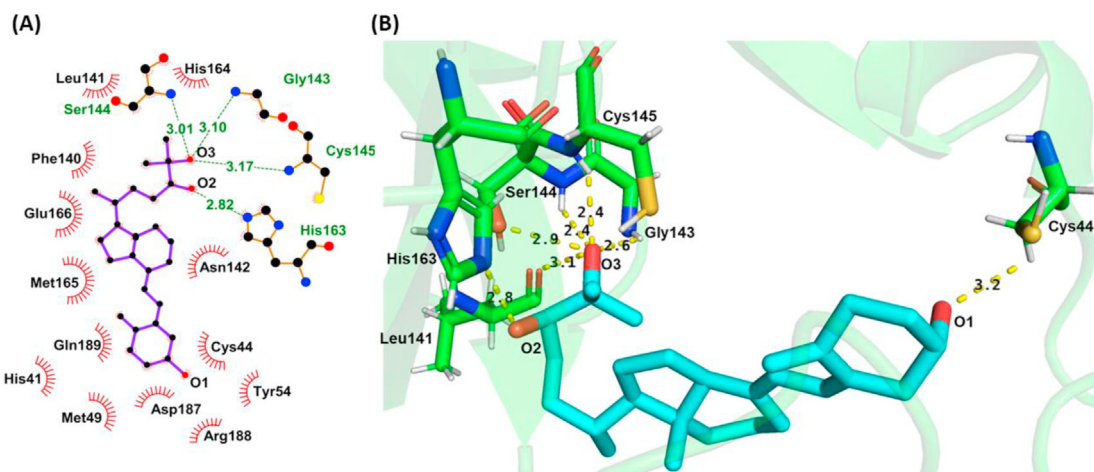


Figure 6. Molecular docking of J11 and SARS-CoV-2 M^{pro}. (A) Ligplot image showing both hydrogen and hydrophobic interactions by J11 and M^{pro}, and (B) Docking pose of J11 against M^{pro}.

of M^{pro}. When docking experiments were performed at pH 4, 5, 6, 7, and 8, it was assumed that all acidic amino acids (Asp and Glu) were deprotonated, while basic amino acids (Arg, Lys, and Cys) were protonated in this pH range. In addition, the protonation states of catalytic His41 and Cys145 were not changed. The protonation state of all other 12 His residues present in the protein changes by changing the partial charge on the atoms of the titratable residue. Moreover, all important domains of M^{pro}, including domains 1 and 2 affecting substrate binding to M^{pro} and domain 3 affecting dimerization, become unstable as the pH becomes acidic or basic. Finally, the correct orientation of the catalytic dyad His41 and Cys145 was only observed at pH 7, but a distorted or wrong orientation was present at all pH values except pH 7. Therefore, in this study, the amino acid residues used in the docking experiments included His41, Cys44, Leu141, Gly143, Asn142, Gly143, Ser144, Cys145, His163, His164, Met165, Glu166, Arg188, and Gln189 as active sites (Figure 3).

Because the purpose of this study was to focus on sterol-like components, the structure-function relationship of 13 sterol-like components identified by MS was further evaluated. The protein-ligand docking model based on the binding affinity of iGemdock showed that the three sterol-like components of RevX extract, clionasterol (J3), 2,7,12-trihydroxycholan-24-oic acid (J4) and 24,25-dihydroxycholecalciferol (J11), have an overall overlap with the active cavity of GC376 (Figures 4, 5, and 6). Figures 4, 5, and 6 show the 2D and 3D structures of the docking ligand molecules. The docked ligand molecules interact strongly with some residues around the active site of GC373, mainly through hydrophobic interactions and hydrogen bonds. The key interaction between the three newly discovered sterol-like components and SARS-CoV-2 M^{pro} was also analyzed.

Clionasterol (J3) forms hydrophobic interactions with Met165, Glu166, Leu167, Pro168, Gln189, Ala191, and Gln192. The hydroxyl group at the C3 site forms hydrogen bonds with the backbone amide groups of Gly143, Ser144, and Cys145 and the carbonyl oxygen of Leu141 and Ser144 (Figure 4).

2,7,12-Trihydroxycholan-24-oic acid (J4) forms hydrogen bonds with His41, Cys145, His163, His164, and Gln189 and hydrophobic interactions with His41, Met 49, Tyr54, Leu141, Ser144, Met165, Glu166, Arg188, and Gln189 in the active site (Figure 5). The O1 hydroxyl group at the C3 site of J4 forms hydrogen bonds with Nε2 of His163 and the amide group of Cys145, and the O2 hydroxyl group at the C7 position forms a hydrogen bond with the sulfhydryl group of Cys145. The O3 hydroxyl group at the C12 site forms hydrogen bonds with Nε2 of His41 and the carbonyl oxygen of His164. The O4 of carboxylate oxygen at the C24 site forms a hydrogen bond with the amide group of Gln189.

Additionally, 24,25-dihydroxycholecalciferol (J11) binds to Cys44, Phe140, Asn142, Met165, Glu166, Asp187, and Gln189 in the GC376-M^{pro} cavity to form hydrophobic interactions and forms hydrogen bonds with Cys44, Leu141, Gly143, Ser144, Cys145, and His163 (Figure 6). The O1 hydroxyl atom at the C3 site of J11 forms a hydrogen bond with Cys44. The O2 hydroxyl group at the C24 position forms a hydrogen bond with Nε2 of His163, and the O3 hydroxyl group at the C25 site forms hydrogen bonds with the amide groups of Gly143, Ser144, and Cys145 and the carbonyl oxygen of Leu141 and His163.

As a common source of nutrients and biologically active compounds, sorghum's variety of biological activities, including anti-oxidation, scavenging free radical, anti-cancer, heart prevention, antibacterial, antiviral, and neuroprotective abilities have been proven. Increasing evidences has also shown that some of the main components in sorghum, such as bioflavones and glycyrrhetic acid, have significant antiviral activity on DNA virus such as human cytomegalovirus and RNA viruses such as SARS-CoV, Ebola virus, and human immunodeficiency virus (Lü et al., 2012; Russo et al., 2020; Ryu et al., 2010). In this study, we report the *in vitro* inhibition test of the RevX solution extract on SARS-CoV-2 M^{pro} and the results of molecular docking of putative candidates. The results show that the solid fraction can strongly inhibit the hydrolytic activity of M^{pro}, which indicates that the solid fraction might prevent the replication of SARS-CoV-2 by inhibiting the enzymatic activity of M^{pro} (Shaito et al., 2020; Wang et al., 2020). The molecular docking of MS identified components shows that the three sterol-like compounds are suitable for the putative active site pocket. COVID-19 is a complex, multi-organ, and heterogeneous severe case that is often accompanied by inflammation in a hypercoagulable state (Chauhan et al., 2020; Cordon-Cardo et al., 2020). In view of the need for supportive treatments for COVID-19, the RevX solution extract may be suitable for COVID-19 patients with chronic diseases such as cardiovascular disease, stroke, hypertension, diabetes and obesity, by relieving the main symptoms of COVID-19 and other underlying health problems.

4. Conclusion

In summary, our analysis of fermented sorghum RevX extract for use in inhibiting SARS-CoV-2 M^{pro} showed that the bioactive components in RevX solution have antiviral activity. GC-MS analysis identified 80 main components of various structural classes from more than 300 compounds, including 13 sterol-like compounds. Docking simulation results of 13 sterol-like compounds revealed 3 compounds that may interact with the protein's active site pocket. Further identification of putative bioactive components and studies of RevX solution as adjunctive therapy are ongoing.

Declarations

Author contribution statement

Feng-Pai Chou, Huynh Nguyet Huong Giang, Sheng-Cih Huang: Performed the experiments; Analyzed and interpreted the data.

Chia-Chun Liu: Contributed reagents, materials, analysis tools or data. Hsiu-Fu Hsu: Conceived and designed the experiments; Contributed reagents, materials, analysis tools or data; Wrote the paper.

Tung-Kung Wu: Conceived and designed the experiments, Wrote the paper.

Funding statement

This work was supported by the Center for Emergent Functional Matter Science and the Center for Intelligent Drug Systems and Smart Bio-devices (IDS²B) of National Yang Ming Chiao Tung University from The Featured Areas Research Center Program within the framework of the Higher Education Sprout Project by the Ministry of Education (MOE) in Taiwan.

Data availability statement

Data will be made available on request.

Declaration of interests statement

The authors declare no conflict of interest.

Additional information

No additional information is available for this paper.

References

- Cardoso, L.D.M., Pinheiro, S.S., Martino, H.S.D., Pinheiro-Sant'Ana, H.M., 2017. Sorghum (*Sorghum bicolor* L.): nutrients, bioactive compounds, and potential impact on human health. *Crit. Rev. Food Sci. Nutr.* 52, 372–390.
- Chauhan, A.J., Wiffen, L.J., Brown, T.P., 2020. COVID-19: a collision of complement, coagulation and inflammatory pathways. *J. Thromb. Haemostasis* 189, 2110–2117.
- Chen, L.L., Chen, S., Gui, C.S., Shen, J., Shen, X., Jiang, H., 2006. Discovering severe acute respiratory syndrome coronavirus 3CL protease inhibitors: virtual screening, surface Plasmon resonance, and fluorescence resonance energy transfer assays. *J. Biomol. Screen* 118, 915–921.
- Chojnacka, K., Witek-Krowiak, A., Skrzypczak, D., Mikula, K., Mlynarz, P., 2020. Phytochemicals containing biologically active polyphenols as an effective agent against Covid-19-inducing coronavirus. *J. Funct. Foods* 73, 104146.
- Cordon-Cardo, C., Pujadas, E., Wajsborg, A., Sebra, R., Patel, G., Firpo-Betancourt, A., Fowkes, M., Sordillo, E., Paniz-Mondolfi, A., Gregory, J., Krammer, F., Simon, V., Isola, L., Soon-Shiong, P., Aberg, J.A., Fuster, V., Reich, D.L., 2020. COVID-19: staging of a new disease comment. *Cancer Cell* 38, 594–597.
- DeLano, W.L., 2002. PyMOL: an open-source molecular graphics tool. *CCP4 Newsl. Protein Crystallogr.* 40, 82–92.
- Ding, H., Deng, W., Ding, L., Ye, X., Yin, S., Huang, W., 2020. Glycyrrhetic acid and its derivatives as potential alternative medicine to relieve symptoms in nonhospitalized COVID-19 patients. *J. Med. Virol.* 92, 2200–2204.
- Du, L., He, Y., Zhou, Y., Liu, S., Zhang, B.-J., Jiang, S., 2009. The spike protein of SARS-CoV - a target for vaccine and therapeutic development. *Nat. Rev. Microbiol.* 7, 226–236.
- Du, Q.-S., Wang, S.-Q., Zhu, Y., Wei, D.-Q., Guo, H., Sirois, S., Chou, K.-C., 2004. Polyprotein cleavage mechanism of SARS CoV Mpro and chemical modification of the octapeptide. *Peptides* 25, 1857–1864.
- Egbuna, C., Shashank Kumar, S., Ifemeje, J.C., Ezzat, S.M., Kaliyaperumal, S. (Eds.), 2020. Plant secondary metabolites as lead compounds for the production of potent drugs in: *Phytochemicals as Lead Compounds for New Drug Discovery*.
- Fehr, A.R., Perlman, S., 2015. Coronaviruses: an overview of their replication and pathogenesis. In: Maier, H.J., Bickerton, E., Britton, P. (Eds.), *Coronaviruses. Methods Mol. Biol.*, 1282 Springer, pp. 1–23.
- Fu, L., Ye, F., Feng, Y., Yu, F., Wang, Q., et al., 2020. Both Boceprevir and GC376 efficaciously inhibit SARS-CoV-2 by targeting its main protease. *Nat. Commun.* 11, 4417.
- Ge, X.Y., Li, J.L., Yang, X.L., et al., 2013. Isolation and characterization of a bat SARS-like coronavirus that uses the ACE2 receptor. *Nature* 503, 535–538.

- Gordon, D.E., Hiatt, J., Bouhaddou, M., Rezelj, V.V., Ulferts, S., Braberg, H., Jureka, A.S., Obernier, K., Guo, J.Z., Batra, J., et al., 2020. Comparative host-coronavirus protein interaction networks reveal pan-viral disease mechanisms. *Science* 370, eabe9403.
- Grant, W.B., Lahore, H., McDonnell, S.L., Baggerly, C.A., French, C.B., Aliano, J.L., Bhattoa, H.P., 2020. Evidence that vitamin D supplementation could reduce risk of influenza and COVID-19 infections and deaths. *Nutrients* 12, E988.
- Hartenian, E., Nandakumar, D., Lari, A., Ly, M., Tucker, J.M., Glaunsinger, B.A., 2020. The molecular virology of coronaviruses. *J. Biol. Chem.* 295, 12910–12934.
- Hilgenfeld, R., 2014. From SARS to MERS: crystallographic studies on coronaviral proteases enable antiviral drug design. *FEBS J.* 281, 4085–4096.
- Hsu, K.C., Chen, Y.F., Lin, S.R., Yang, J.M., 2011. iGEMDOCK: a graphical environment of enhancing GEMDOCK using pharmacological interactions and post-screening analysis. *BMC Bioinf.* 12, S33.
- Kamath, V., Niketh, S., Chandrashekar, A., Rajini, P.S., 2007. Chymotryptic hydrolysates of α -kafirin, the storage protein of sorghum (*Sorghum bicolor*) exhibited angiotensin converting enzyme inhibitory activity. *Food Chem.* 100, 306–311.
- Kneller, D.W., Phillips, G., O'Neill, H.M., Tan, K., Joachimiak, A., Coates, L., Kovalevsky, A., 2020. Room temperature X-ray crystallography reveals oxidation and reactivity of cysteine residues in SARS-CoV-2 3CL Mpro: insights for enzyme mechanism and drug design. *IUCr J.* 7, 1028–1035.
- Li, G., Clercq, E.D., 2020. Therapeutic options for the 2019 novel coronavirus (2019-nCoV). *Nat. Rev. Drug Discov.* 19, 149–150.
- Lü, J.M., Yan, S.Y., Jamaluddin, S.H., 2012. Ginkgolic acid inhibits HIV protease activity and HIV infection in vitro. *Med. Sci. Mon. Int. Med. J. Exp. Clin. Res.* 18, BR293–298.
- Lin, C.J., 2021. Effect of RevX solution adjunct to standard therapy in a patient with metastatic lung adenocarcinoma: a case report. *Int. J. Case Rep.* 5, 238.
- Lipinski, C.A., Lombardo, F., Dominy, B.W., Feeney, P.J., 2011. Experimental and computational approaches to estimate solubility and permeability in drug discovery and development settings. *Adv. Drug Deliv. Rev.* 46, 3–26.
- Lu, R., Zhao, X., Li, J., Niu, P., Yang, B., Wu, H., et al., 2020. Genomic characterisation and epidemiology of 2019 novel coronavirus: implications for virus origins and receptor binding. *Lancet* 395, 565–574.
- Meng, X.-Y., Zhang, H.-X., Mezei, M., Cui, M., 2011. Molecular Docking: a Powerful Approach for Structure-Based Drug Discovery, 7, pp. 146–157.
- Muriu, J.I., Njoka-Njiru, E.N., Tuitoek, J.K., Nanua, J.N., 2002. Evaluation of sorghum (*Sorghum bicolor*) as replacement for maize in the diet of growing rabbits (*Oryctolagus cuniculus*). *AJAS (Asian-Australas. J. Anim. Sci.)* 15, 565–569.
- Oh, K.K., Adnan, M., Cho, D.H., 2020. Network pharmacology of bioactives from *Sorghum bicolor* with targets related to diabetes mellitus. *PLoS One* 15, e0240873.
- Painter, W.P., Holman, W., Bush, J.A., Almazedi, F., Malik, M., Erant, N.C.J.E., et al., 2021. Human safety, tolerability, and pharmacokinetics of molnupiravir, a novel broad-spectrum oral antiviral agent with activity against SARS-CoV-2. *Antimicrob. Agents Chemother.* 65, e02428-02420.
- Russo, M., Moccia, S., Spagnuolo, C., Tedesco, I., Russo, G.L., 2020. Roles of flavonoids against coronavirus infection. *Chem. Biol. Interact.* 328, 109211.
- Rut, W., Groborz, K., Zhang, L., Sun, X., Zmudzinski, M., Pawlik, B., Wang, X., Jochmans, D., Neyts, J., Mlynarski, W., Hilgenfeld, R., Drag, M., 2021. SARS-CoV-2 Mpro inhibitors and activity-based probes for patient-sample imaging. *Nat. Chem. Biol.* 17, 222–228.
- Ryu, Y.B., Jeong, H.J., Kim, J.H., Kim, Y.M., Park, J.Y., Kim, D., Nguyen, T.T., Park, S.J., Chang, J.S., Park, K.H., Rho, M.C., Lee, W.S., 2010. Biflavonoids from *Torreya nucifera* displaying SARS-CoV 3CLpro inhibition. *Bioorg. Med. Chem.* 18, 7940–7947.
- Saha, A., Sharma, A.R., Bhattacharya, M., Sharma, G., Lee, S.-S., Chakraborty, C., 2020. Probable molecular mechanism of remdesivir for the treatment of COVID-19: need to know more. *Arch. Med. Res.* 51, 585–586.
- Shaito, A., Thuan, D.T.B., Phu, H.T., Nguyen, T.H.D., Hasan, H., Halabi, S., Abdelhady, S., Nasrallah, G.K., Eid, A.H., Pintus, G., 2020. Herbal medicine for cardiovascular diseases: efficacy, mechanisms, and safety. *Front. Pharmacol.* 11, 422.
- Shih, C.-H., Siu Ng, R., Wong, E., Chiu, L.C.M., Chu, I.K., Lo, C., 2007. Quantitative analysis of anticancer 3-deoxyanthocyanidins in infected sorghum seedlings. *J. Agric. Food Chem.* 55, 254–259.
- Tan, J., Koen, H.G., et al., 2005. pH-dependent conformational flexibility of the SARS-CoV main protease (Mpro) dimer: molecular dynamics simulations and multiple X-ray structure analyses. *J. Mol. Biol.* 354, 25–40.
- Ullrich, S., Nitsche, C., 2020. The SARS-CoV-2 main protease as drug target. *Bioorg. Med. Chem. Lett* 30, 127377.
- Vuong, W., Khan, M.B., Fischer, C., Arutyunova, E., Lamer, T., 2020. Feline coronavirus drug inhibits the main protease of SARS-CoV-2 and blocks virus replication. *Nat. Commun.* 11, 4282.
- Wang, Z., Zhang, P., Wang, Q., Sheng, X., Zhang, J., Lu, X., Fan, X., 2020. Protective effects of Ginkgo biloba Dropping Pills against liver ischemia/reperfusion injury in mice. *Chin. Med.* 151, 122.
- Wen, C.C., Kuo, Y.H., Jan, J.T., Liang, P.H., Wang, S.Y., et al., 2007. Specific plant Terpenoids and Lignoids possess potent antiviral activities against severe acute respiratory syndrome coronavirus. *J. Med. Chem.* 50, 4087–4095.
- Yang, H., Rao, Z., 2021. Structural biology of SARS-CoV-2 and implications for therapeutic development. *Nat. Rev. Microbiol.* 19, 685–700.
- Yang, L., Browning, J.D., Awika, J.M., 2009. Sorghum 3-deoxyanthocyanins possess strong phase II enzyme inducer activity and cancer cell growth inhibition properties. *J. Agric. Food Chem.* 57, 1797–1804.
- Zhang, L., Lin, D., Sun, X., Curth, U., Drosten, C., Sauerhering, L., Becker, S., Rox, K., Hilgenfeld, R., 2020a. Crystal structure of SARS-CoV-2 main protease provides a basis for design of improved α -ketoamide inhibitors. *Science* 368, 409–412.
- Zhang, L., Lin, D., Sun, X., et al., 2020b. Crystal structure of SARS-CoV-2 main protease provides a basis for design of improved α -ketoamide inhibitors. *Science* 368, 409–412.